J. Fluid Mech. (1994), *vol.* 281, *pp.* 137–158

Biflagellate gyrotaxis in a shear flow

By M. S. JONES, L. LE BARON AND T. J. PEDLEY
Department of Applied Mathematical Studies, University of Leeds, Leeds, LS2 9JT, UK

(Received 2 July 1993 and in revised form 11 June 1994)

A flagellated, bottom-heavy micro-organism's swimming direction in a shear flow is determined from a balance between the gravitational and viscous torques (gyrotaxis). Hitherto, the cell has been assumed to be a spheroid and the flagella have been neglected. Here we use resistive-force theory to calculate both the magnitude and the direction of a biflagellate cell's swimming velocity and angular velocity relative to the fluid when there is an arbitrary linear flow far from the cell. We present an idealized model for the flagellar beat but, in calculating the velocity of the fluid relative to an element of a flagellum, the presence of the cell body is not neglected. Results are given for the case of a spherical cell body whose flagella beat in a vertical plane, when the ambient linear flow is in the same vertical plane. Results show that resistive-force theory can be used for organisms where the cell body has significant effect on the flow past the flagella and that the viscous torque on the flagella is a significant term in the torque balance equations. A model is presented for the calculation of a cell's velocity and angular velocity in a shear flow which is valid up to high magnitudes of rate of strain or vorticity. The main application of the results will be to modify a recent continuum model for suspensions of gyrotactic micro-organisms (Pedley & Kessler 1990).

1. Introduction

Many biflagellate algal cells, from genera such as *Chlamydomonas* and *Dunaliella*, have a body whose shape is roughly that of a prolate spheroid, and are propelled by a pair of long thin flagella attached to the body at one end as sketched in figure 1(*a*). The flagella perform a breast-stroke-style motion and propel the body approximately in the direction of its axis of symmetry. The length of a typical cell body is 10–15 μm while the flagella may be 20 μm long. The cell contents are asymmetrically distributed within the cell, so that its centre of mass is displaced towards the rear from the geometrical centre. Such cells are of interest not only because of their great abundance among the phytoplankton of oceans and lakes, where they both form part of the bottom link of the food chain and absorb a large proportion of ambient CO_2, nor only for their biotechnological value, but also because suspensions of them in the laboratory exhibit a fascinating hydrodynamic instability that leads to relatively large-scale (2–10mm) patterns in a process known as bioconvection (Pedley & Kessler 1992). A knowledge of the microhydrodynamics of individual cells is an important stage in the development of a rational continuum model for such suspensions.

The purpose of this paper is to analyse the swimming of a single such cell in a viscous fluid which is itself undergoing a general motion, with vorticity and strain rate in the neighbourhood of the cell. The cell is assumed also to be subjected to an external torque, originating in the examples of interest from the action of gravity

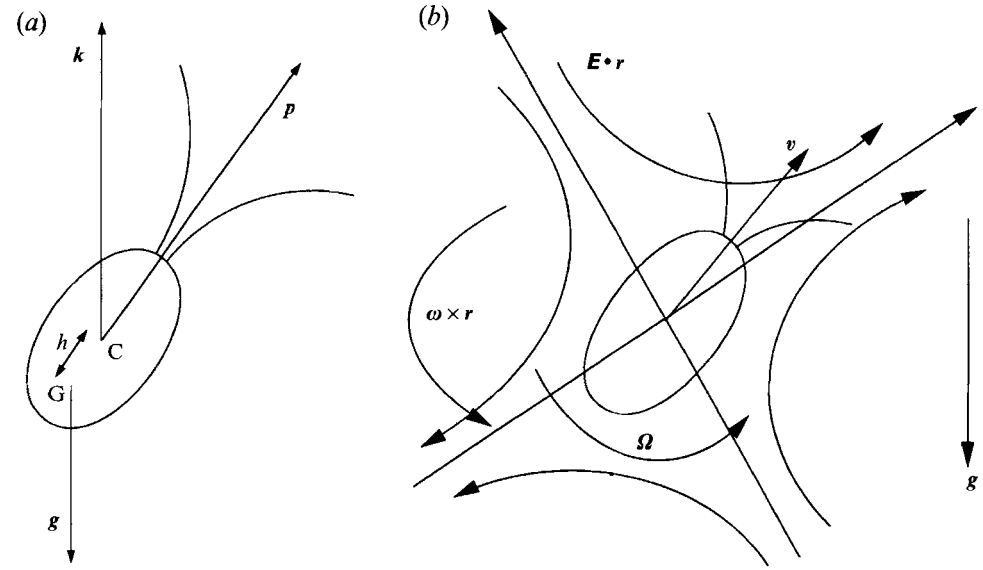

FIGURE 1. (*a*) Sketch of a biflagellate algal cell; $\boldsymbol{p},\boldsymbol{k}$ are unit vectors parallel to the cell axis and vertically upwards respectively; h is the offset of the centre of gravity G from the geometric centre C. (*b*) Cell embedded in a flow containing vorticity $\boldsymbol{\omega}$ and strain rate $\boldsymbol{E}$. The cell's motion is given by its velocity $\boldsymbol{v}$ and angular velocity $\boldsymbol{\Omega}$.

on the cell's asymmetric mass distribution. The equilibrium orientation of a steadily swimming cell, represented by the unit vector $\boldsymbol{p}$ along its major axis, is determined by a balance between gravitational and viscous torques, and the directed locomotion that results is termed gyrotaxis (Kessler 1985). When the orientation is not in equilibrium, its rate of change $\dot{\boldsymbol{p}}$, the component of the cell's angular velocity perpendicular to $\boldsymbol{p}$, is still determined by the torque balance.

The previous analyses of gyrotaxis, incorporated into the continuum models of cell suspensions, have assumed that the viscous torque on a cell is effectively the same as the viscous torque on the spheroidal body alone (Pedley, Hill & Kessler 1988; Pedley & Kessler 1990). Using the theory of Jeffery (1922), to calculate the torque on a spheroid, these authors found that

$$\dot{\boldsymbol{p}} = \frac{1}{2B}[\boldsymbol{k} - (\boldsymbol{k}\cdot\boldsymbol{p})\,\boldsymbol{p}] + \tfrac{1}{2}\,\boldsymbol{\omega}\times\boldsymbol{p} + \alpha_0\,\boldsymbol{p}\cdot\boldsymbol{E}\cdot[\boldsymbol{I} - \boldsymbol{p}\,\boldsymbol{p}^{\mathrm{T}}], \tag{1.1}$$

where $\boldsymbol{\omega}$, $\boldsymbol{E}$ are the vorticity and the strain-rate of the ambient flow respectively, $\boldsymbol{k}$ is a unit vector directed vertically upwards, $\boldsymbol{I}$ is the identity tensor and α_0 is a measure of the cell's eccentricity. The constant B is the 'gyrotactic reorientation time' given by

$$B = \frac{\mu v \alpha_\perp}{2mgh}, \tag{1.2}$$

where μ is the fluid viscosity, g is the gravitational acceleration, v, m are the cell's volume and mass respectively, h is the displacement of the centre of mass (CG in figure 1*a*) and $\alpha_\perp$ is a dimensionless number dependent on α_0.

The previous models also assumed that the beating flagella result in a constant swimming speed, V_s, and that the swimming direction is parallel to the body axis, $\boldsymbol{p}$. In fact, the presence of the beating flagella in an ambient shear flow means that the swimming speed relative to the ambient fluid varies cyclically (forwards during

the effective stroke and backwards during the recovery stroke), that the swimming direction is not in general parallel to $\boldsymbol{p}$ and, especially, that the viscous torque is not the same as that on the body alone. We use a microhydrodynamic analysis to examine the magnitude of these effects, and to determine the extent to which the latest continuum model (Pedley & Kessler 1990) needs to be changed as a result.

We shall take a frame of reference with origin at the centre of the cell, which is assumed to be embedded in a general linear flow. Thus, if the cell's swimming velocity relative to the fluid is $\boldsymbol{v}$, the velocity field in the fluid far from the cell will be taken to be

$$\boldsymbol{u}_\infty = -\boldsymbol{v} + \tfrac{1}{2}\,\boldsymbol{\omega} \times \boldsymbol{r} + \boldsymbol{E} \cdot \boldsymbol{r}, \tag{1.3}$$

where $\boldsymbol{r}$ is the position vector (see figure 1*b*). The angular velocity of the cell is $\boldsymbol{\Omega}$.

The Reynolds number of the motion of the cell as well as of the flagella is small, so inertia is negligible. It follows that the total force and the total torque acting on the cell are both zero at all times during the flagellar beat. The forces are made up of the viscous force on the body, the viscous force on the flagella and the gravitational (negative buoyancy) force on the cell as a whole, and similarly for the torques. In fact we shall ignore the gravitational force (not torque) on the cell on the grounds that it is small compared with the viscous thrust/drag forces; this follows from the observation that the sedimentation speed of dead cells (e.g. of *C. nivalis*) is about 2 μm s^{-1}while the swimming speed of live cells is about 70 μm s^{-1}.

The most accurate methods for computing the viscous forces and torques on the cell are those that are equivalent to a complete solution of the Stokes equations at every instant as the surface of the body-plus-flagella changes shape. The best developed is the boundary integral/element method of Phan-Thien, Tran-Cong & Ramia (1987), Ramia (1991) and Ramia, Tullock & Phan-Thien (1993), while the immersed boundary method has been used for two-dimensional models of swimming biflagellate algae (Fauci & Peskin 1988). Slender-body theory (Lighthill 1976; Higdon 1979) gives a rational approximation to the exact solution but requires complicated analytical expressions for the image system of a force singularity in the cell body. Implementing any of these methods here would be extremely time-consuming and computer-intensive, and would be unlikely to yield simple formulae for the forces and torques (or, equivalently, for the components of the cell's velocity and angular velocity).

In this paper, therefore, the viscous forces and torques on the flagella will be calculated using resistive-force theory (Gray & Hancock 1955) in which the normal and tangential components of force exerted on an element of a flagellum are taken to be directly proportional to the normal and tangential components of the fluid's velocity relative to that element. Resistive-force theory is a crude approximation of the true flagellar hydrodynamics, but has been shown not to give grossly inaccurate results if sensible choices are made of the constants of proportionality, at least for the swimming of spermatozoa (Lighthill 1976; Winet & Jahn 1972).

In the analyses of spermatozoa, the relative velocity $\boldsymbol{u}_{\rm rel}$ has been taken to be the difference between the far-field velocity $\boldsymbol{u}_\infty$ (equation (1.3) or, more usually, $\boldsymbol{u}_{\rm rel} = -\boldsymbol{v}$) and the active velocity $\boldsymbol{v}_{\rm flag}$ of the element of flagellum relative to the frame of reference. The presence of the sperm head is neglected because the sperm tail is very long compared with the head. In the present case, however, the flagella have a length comparable with the body diameter and therefore the deflection of the far-field velocity by the body must be taken into consideration in calculating $\boldsymbol{u}_{\rm rel}$.

The theoretical model is described fully in § 2 where the deflection of the far field is given explicitly for a spherical body. The choice of resistance coefficients is discussed in § 3. A further necessary ingredient of the model is a quantitative description of the pattern of the flagellar beat; § 4 describes the observations of the three-dimensional beat pattern of *Chlamydomonas* made by Ruffer & Nultsch (1985), followed by the idealized planar beat pattern assumed for the present work. Implementation of the model for the special case in which the ambient straining motion is two-dimensional, the vorticity is perpendicular to the plane of the strain, and both the flagellar beat and the gravity vector lie in that plane, is described in detail in § 5. Results are given in § 6 and the discussion in § 7 focuses on the conditions under which the old model of gyrotaxis, with $\boldsymbol{v}$ parallel to $\boldsymbol{p}$ and $\dot{\boldsymbol{p}}$ given by equation (1.1) for some value of B, can be used with reasonable accuracy in a continuum model of a suspension of cells.

2. General model

The cell's major axis, $\boldsymbol{p}$, points along the direction of the cell's propulsion; figure 1(*a*) shows the body axis and the gravity axis. The geometric centre C and the centre of mass G lie on this axis, and the two flagella are assumed to connect to the body at a single point, also on the axis. The centre of mass is displaced a distance h from C.

Because inertia is assumed to be negligible, the orientation and motion of the cell are given by the force and torque balances on it. The contributions to the force and torque are those due to (*a*) gravity and (*b*) viscosity acting on the cell body and on the flagella respectively:

$$\boldsymbol{F}_{\text{grav}} + \boldsymbol{F}_{\text{body}} + \boldsymbol{F}_{\text{flag}} = 0 \tag{2.1}$$

and

$$\boldsymbol{L}_{\text{grav}} + \boldsymbol{L}_{\text{body}} + \boldsymbol{L}_{\text{flag}} = 0. \tag{2.2}$$

As mentioned in § 1, observations show that the sedimentation speed of dead cells is much less than the swimming speed of live cells. We may therefore neglect the force due to gravity, $\boldsymbol{F}_{\text{grav}}$. The gravitational couple, $\boldsymbol{L}_{\text{grav}}$, makes a significant contribution, however, and is given by

$$\boldsymbol{L}_{\text{grav}} = h\boldsymbol{p} \times mg\boldsymbol{k}. \tag{2.3}$$

The sign of the couple is chosen to correspond with the geometry of the algal cells previously considered by Pedley & Kessler (1987).

When calculating the contributions to the force and torque due to the body, $\boldsymbol{F}_{\text{body}}$ and $\boldsymbol{L}_{\text{body}}$ respectively, we neglect the presence of the flagella attached to the body and any flows produced directly by the beating flagella. The contributions are then the hydrodynamic force and torque on the body in Stokes flow. This is a classical problem for spherical and spheroidal body shapes (Kim & Karrila 1991).

It remains to calculate the contribution to the force and torque due to the flagella, $\boldsymbol{F}_{\text{flag}}$ and $\boldsymbol{L}_{\text{flag}}$. We choose to use resistive force theory (Gray & Hancock 1955; Lighthill 1976). This says that $\mathrm{d}\boldsymbol{F}_{\text{flag}}$, the viscous force exerted upon an element $\boldsymbol{t}\,\mathrm{d}s$ of a flagellum, where $\boldsymbol{t}$ is the unit vector tangential to the flagellum, is linearly related to the velocity of the fluid relative to the element, $\boldsymbol{u}_{\text{rel}}$:

$$\mathrm{d}\boldsymbol{F}_{\text{flag}} = \mu\{K_N(\boldsymbol{u}_{\text{rel}} \cdot \boldsymbol{n})\,\boldsymbol{n}\,\mathrm{d}s + K_T(\boldsymbol{u}_{\text{rel}} \cdot \boldsymbol{t})\,\boldsymbol{t}\,\mathrm{d}s\}, \tag{2.4}$$

where $\boldsymbol{n}$ is a unit vector normal to $\boldsymbol{t}$, in the same plane as $\boldsymbol{u}_{\text{rel}}$ and $\boldsymbol{t}$†, K_N and

† Thus $(\boldsymbol{u}_{\text{rel}} \cdot \boldsymbol{n})\boldsymbol{n} = \boldsymbol{u}_{\text{rel}} - (\boldsymbol{u}_{\text{rel}} \cdot \boldsymbol{t})\boldsymbol{t}$.

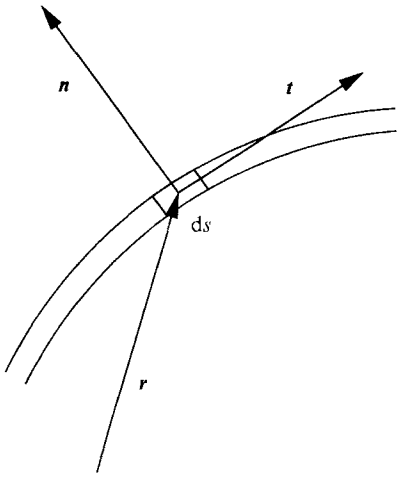

FIGURE 2. Position of an element $t\,ds$ of a flagellum.

K_T are dimensionless resistance coefficients in the normal and tangential directions respectively and μ is the viscosity of water (figure 2).

In order to calculate the viscous force upon the element of the flagellum, it can be seen that we require the velocity of the fluid relative to the element, $\boldsymbol{u}_{\text{rel}}$. The velocity of the fluid, $\boldsymbol{u}$, is measured at the position of the element $\mathrm{d}s$ assuming that the presence of the flagellum has no effect upon the fluid flow. For a spherical body in a general flow field, this is made up of three parts: the flow due to the translation of the body, the flow due to the vorticity of the ambient flow and the rotation of the body, and the flow due to any ambient straining motion. The flow past the body is then

$$\boldsymbol{u} = \boldsymbol{u}_{\text{tran}} + \boldsymbol{u}_{\text{rot}} + \boldsymbol{u}_{\text{str}}, \tag{2.5}$$

where the flow due to the translation is

$$\boldsymbol{u}_{\text{tran}} = -\boldsymbol{v}\left(1 - \frac{3a}{4r} - \frac{a^3}{4r^3}\right) + \frac{(\boldsymbol{v}\cdot\boldsymbol{r})}{r^2}\,\boldsymbol{r}\,\frac{3a}{4r}\left(1 - \frac{a^2}{r^2}\right), \tag{2.6}$$

the flow due to the vorticity and rotation is

$$\boldsymbol{u}_{\text{rot}} = \frac{1}{2}\,\boldsymbol{\omega}\times\boldsymbol{r}\left(1 - \frac{a^3}{r^3}\right) + \boldsymbol{\Omega}\times\boldsymbol{r}\,\frac{a^3}{r^3} \tag{2.7}$$

and that due to strain is

$$\boldsymbol{u}_{\text{str}} = \boldsymbol{E}\cdot\boldsymbol{r}\left(1 - \frac{a^5}{r^5}\right) - \frac{5}{2}\,\boldsymbol{r}\,\frac{(\boldsymbol{r}\cdot\boldsymbol{E}\cdot\boldsymbol{r})}{r^2}\,\frac{a^3}{r^3}\left(1 - \frac{a^2}{r^2}\right) \tag{2.8}$$

where a is the radius of the cell body.

The velocity of an element of flagellum, $\boldsymbol{v}_{\text{flag}}$, is given by

$$\boldsymbol{v}_{\text{flag}} = \boldsymbol{\Omega}\times\boldsymbol{r} + \dot{\boldsymbol{r}}, \tag{2.9}$$

where $\boldsymbol{\Omega}$ is the angular velocity of the body and $\boldsymbol{r}$ is the position vector of the element relative to a frame of reference rotating with the body with origin at its geometric centre, C. The velocity of the fluid relative to the element, $\boldsymbol{u}_{\text{rel}}$, is then given by

$$\boldsymbol{u}_{\text{rel}} = \boldsymbol{u} - \boldsymbol{v}_{\text{flag}}. \tag{2.10}$$

The viscous force exerted upon the element can now be calculated and, by quadrature, the viscous force and torque on the entire flagella can also be found. This enables a calculation of the velocity and angular velocity of the cell to be made at any instant. By averaging the results over the flagellar beat, the average velocity and angular velocity are found.

3. Choice of resistance coefficients

An important consideration in the use of resistive-force theory is the choice of the resistance coefficients, K_N and K_T. Two pairs of coefficients have been proposed: those due to Gray & Hancock (1955) and those due to Lighthill (1976).

Gray & Hancock, in their original formulation of resistive force theory, gave the values of the resistive coefficients as

$$K_N = \frac{4\pi}{\ln(2q/b) + \frac{1}{2}} \tag{3.1}$$

and

$$K_T = \frac{2\pi}{\ln(2q/b) - \frac{1}{2}}, \tag{3.2}$$

where q is a characteristic length indicating the range of influence exerted by a force acting at the element $\boldsymbol{t}ds$ of a flagellum and b is the cross-sectional radius of the flagellum. Gray & Hancock thought that a high degree of accuracy in the choice of q was not important and, in applying the theory to a long spermatazoon, chose q equal to the flagellar wavelength, λ.

Lighthill argued that q had to be small in relation to λ for resistive force theory to be more accurate. He proposed that a more realistic figure was $q = 0.09\lambda$ but found that, when this was used in the Gray & Hancock coefficients, it produced a ratio of swimming speed to wave propagation speed that was significantly larger than observed. He therefore recalculated the resistive coefficients for small q and found that K_N should still be given by (3.1) but K_T should be replaced by

$$K_T = \frac{2\pi}{\ln(2q/b)} \tag{3.3}$$

with $q = 0.09\lambda$.

In both cases, the coefficients were formulated on the assumption that the flagellum was infinitely long. This is the zero-thrust case, because there is no head or body to provide an opposing drag, and is typical of organisms such as spermatozoa where the body diameter is small in comparison with the flagellar length. Johnson & Brokaw (1979) found that Lighthill's coefficients gave good agreement with the more accurate slender-body theory even in the non-zero-thrust case when the head provided a significant drag.

Resistive-force theory is crude in its approximation because it takes no account of the interaction between neighbouring elements of the flagella. This is especially significant at the free ends of the flagella and close to the body. In our case, we have a flagellar length comparable to the body diameter; *Chlamydomonas* typically has a body diameter from 10 to 15 μm and flagellar lengths from 20 to 40 μm. In order to assess whether errors in the resistance coefficients are significant or not in this case, we compute two sets of results, one with Gray & Hancock's values and one with Lighthill's.

Another consideration is that the flagella beat in such a way that there are no travelling waves visibly moving down the flagella as in spermatozoa (see § 4). Thus it is not clear how to calculate the flagellar wavelength. We choose to use one flagellar beat as one wave and arbitrarily let the flagellar wavelength be twice the flagellar length. The accuracy of this assumption will have to be assessed subsequently, using a more complete theory.

We will show how the choice of q, b and the resistive force coefficients affects the up-swimming velocity of the organism.

4. Flagellar beat model

It will be necessary in the development of the theory to incorporate a description of the beat pattern of the organism's flagella. We first summarize the observations of Ruffer & Nultsch (1985) for a typical *Chlamydomonas* cell, and then describe our idealized model of the flagellar beat, based upon those observations.

4.1. *Observed flagellar beat*

The beating of *Chlamydomonas* has been described by numerous authors (Ringo 1967; Hyams & Borissy 1978). They observe that the organism swims by using a breast-stroke-like beat divided into two distinct phases, the effective stroke and the recovery stroke. In figure 3(*a*) the phases are clear, though not totally distinct. In the effective stroke, the flagella are extended and brought from an upwards position back towards the body; the relative velocity is mostly normal to the flagellum. In the recovery stroke, a bend travels from the base to the tip of each flagellum causing the tip to move towards the body while returning to its initial position; in this part of the beat there is more tangential relative velocity. The two phases of the beat were observed to overlap, the effective stroke beginning before the recovery stroke had fully extended the flagella and the recovery stroke starting to bend the flagella before the effective stroke had brought them fully back.

The effect of the beat on the motion of the cell is shown in figure 3(*b*). The body moves forwards during the effective stroke and backwards during the recovery stroke. The forward motion during the effective stroke is greater than the backwards motion during the recovery stroke, essentially because K_N exceeds K_T. The net effect is up-swimming, on average. Ruffer & Nultsch also observed that the two strokes typically take place in somewhat different planes, with some bending of parts of the flagella out of the beat plane. The consequence is an anti-clockwise rotation about the cell axis that was observed to take place entirely during the effective stroke.

A *Chlamydomonas* cell typically swims in a helical path. The flagellum at the outer side of the helical spin was observed occasionally to increase its frequency, in comparison with that of the inner flagellum, for short periods of time. This transient acceleration was the main source of asymmetry in the beat pattern. The cells studied by Ruffer & Nultsch beat at frequencies between 40 and 60 Hz, and swam at speeds of between 100 and 200 μm s^{-1}(maximum 240 μm s^{-1}). The rotation rates were in the range 1.4 to 2.5 Hz or 9–15° per beat; asymmetries occurred about once per 20 beats or 2 to 2.5 per rotation.

It would be desirable to use a quantitative description of the observed beat pattern of figure 3 in implementing resistive-force theory. Unfortunately there is an apparent inconsistency in the observations which makes it difficult to do so. This is that the lengths of the flagella as drawn do not remain constant throughout the beat. It might be thought that the non-planar character of the beat could explain the

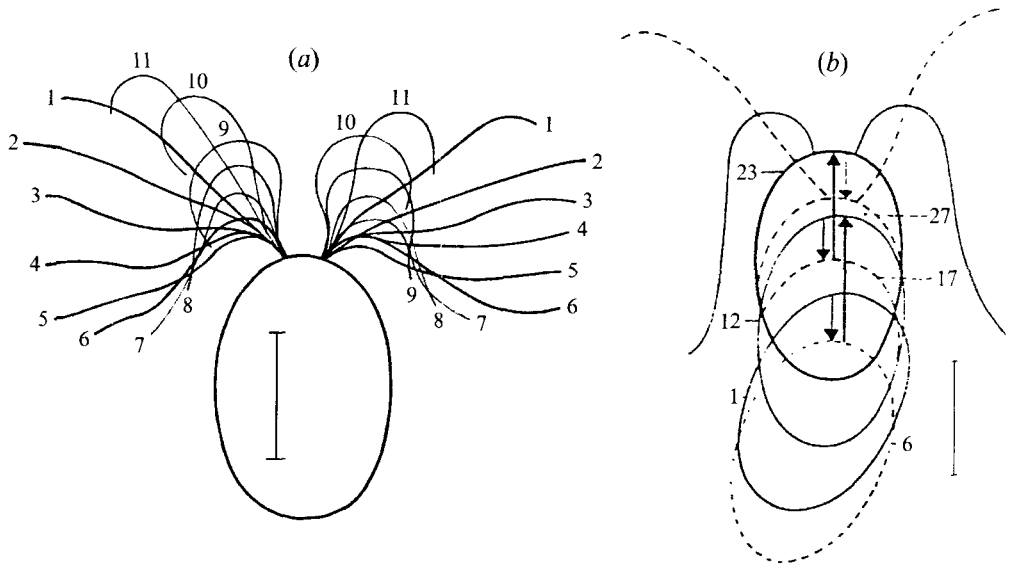

FIGURE 3. (*a*) *C. reinhardtii* mutant 622E. Tracing of one beat cycle of both flagella from a phase-contrast, high-speed film (500 f/s). Film images were magnified 85×. Cell–body schematic. Figures are frame numbers. Bar = 5 μm. Reproduced with permission from Ruffer & Nultsch (1985). (*b*) Position of another cell during three beats. The solid line marks the cell at the end of the forward motion, the dashed line at the end of the backward motion. For the last beat, the position of the flagellum at the beginning of the effective (dashed line) and recovery stroke (solid line) is given. Arrows indicate direction and magnitude of movement. Reproduced with permission from Ruffer & Nultsch (1985).

anomaly, because only a planar projection of the flagella can be drawn at any instant. However, the apparent length changes are too great to be accounted for in this way, given the rather small out-of-plane component of the observed beat. Various ways of adjusting the data can be thought of, such as scaling the measured positions of points on a flagellum by instantaneous recorded length, but they are all essentially arbitrary and would give a spurious biological verisimilitude to the results of our model. Instead, we have devised and used a highly idealized model of the flagellar beat in computing our results, as described below.

4.2. *Idealized flagellar beat model*

We assume that the flagella beat symmetrically in a plane containing the longitudinal body axis. We do not allow for any rotation about the body axis nor model the helical swimming path. We also assume that the effective and recovery strokes are distinct. The model beat starts with the flagella fully extended parallel to the body axis (figure 4*a*: flagella position 1). For the effective stroke, the flagella rotate rigidly about their base (O, in figure 4*a*) until perpendicular to the body axis. The angular velocity of each flagellum about O is taken to be constant throughout the motion. The angle between the flagellum and the body axis $\boldsymbol{p}$ at any stage is denoted by χ. The other flagellum beats symmetrically.

During the recovery stroke, the bending waves propagate up the flagellum from the base to the tip: with reference to figure 4(*b*), the propagation point P is taken to travel in the direction of the body axis, restoring the flagellum to the initial position. The flagellum bends sharply as the wave moves up the axis at a constant speed w.

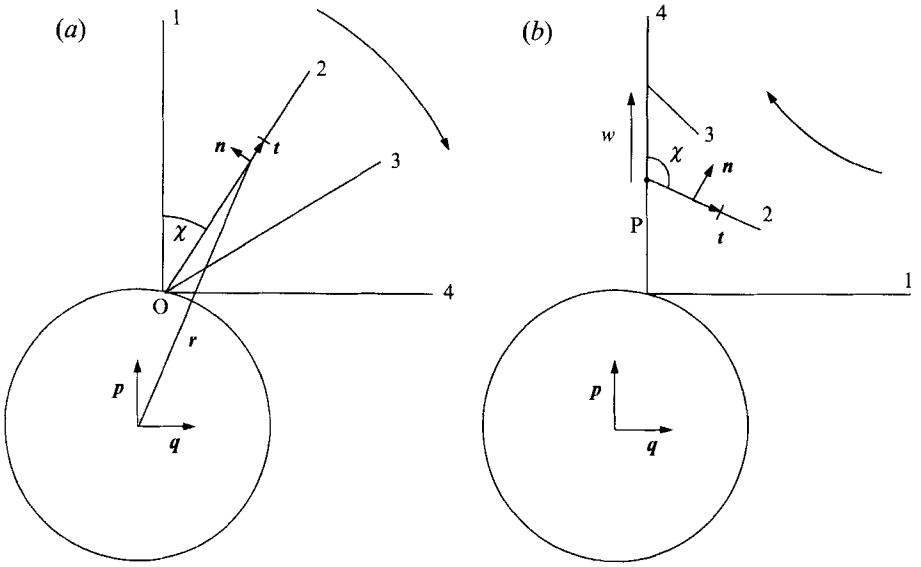

FIGURE 4. (*a*) Idealized effective stroke of one flagellum. Numbers follow the sequence of flagellar positions. A typical element is shown on the flagellum with normal and tangential vectors $\boldsymbol{n}, \boldsymbol{t}$. (*b*) Idealized recovery stroke. The point P propagates along the line of the cell axis with speed w.

We model the changing angle χ between the flagellum and the body axis during the recovery stroke in one of two ways:

(*a*) the angle decreases at a constant angular velocity;

(*b*) the angle is calculated in such a way that the moment about the bending point of the viscous forces acting on the dependent part of the flagellum is zero.

We assume that the beat pattern described above is unchanged by any changes in the ambient flow.

5. Single plane model

Following the specification of the flagellar beat, all the assumptions can be incorporated into the general model. For simplicity, we restrict the calculation of results to a uniplanar case. That is, within the ambient flow, the vorticity is perpendicular to the plane of the strain rate. The flagellar beat plane will coincide with the plane of the strain rate and gravity will also act wholly within that plane (figure 5). In a suitable coordinate system, therefore, we can write

$$\boldsymbol{E} = \begin{pmatrix} e & 0 & 0 \\ 0 & -e & 0 \\ 0 & 0 & 0 \end{pmatrix}, \quad \boldsymbol{\omega} = \begin{pmatrix} 0 \\ 0 \\ \omega \end{pmatrix}, \quad \boldsymbol{g} = -g\boldsymbol{k} = \begin{pmatrix} -g\sin\gamma \\ -g\cos\gamma \\ 0 \end{pmatrix}, \quad \boldsymbol{p} = \begin{pmatrix} \sin\theta \\ \cos\theta \\ 0 \end{pmatrix}. \tag{5.1}$$

Within the coordinate system described above, the gravitational torque becomes

$$\boldsymbol{L}_{\text{grav}} = mgh\sin(\theta - \gamma)\,\boldsymbol{e}_3, \tag{5.2}$$

where $\boldsymbol{e}_3$ is a unit vector in the direction perpendicular to the flow plane (out of the page in figure 5), θ is the angle of the body axis relative to the negative strain rate axis and γ is the angle of the upward vertical relative to this strain axis.

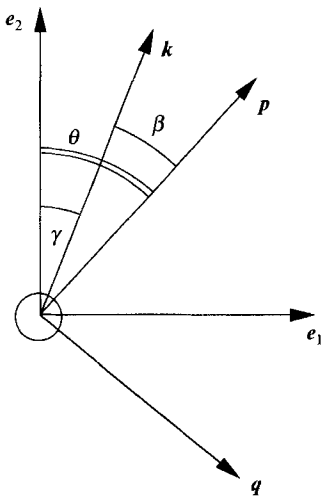

FIGURE 5. The uniplanar model. The body axes $\boldsymbol{p}$ and $\boldsymbol{q}$, the strain axes $\boldsymbol{e}_i$ and gravity axis $\boldsymbol{k}$ (vertically upwards) all lie in the same plane. θ is the angle of the body axis relative to the negative strain rate axis and γ is the angle of the upwards vertical relative to this strain axis.

Our assumption that the body is spherical in shape means that the viscous force and torque upon the body, $\boldsymbol{F}_{\text{body}}$ and $\boldsymbol{L}_{\text{body}}$, are well known:

$$\boldsymbol{F}_{\text{body}} = -6\pi\mu a\boldsymbol{v}, \tag{5.3}$$

$$\boldsymbol{L}_{\text{body}} = -8\pi\mu a^3(\boldsymbol{\Omega} - \tfrac{1}{2}\boldsymbol{\omega}). \tag{5.4}$$

The velocity field for a general linear flow past a spherical body was given in § 2 above. To find the relative velocity of the fluid over the element $\boldsymbol{t}ds$, it remains to define the position vector $\boldsymbol{r}$ and the velocity $\dot{\boldsymbol{r}}$ of the element, relative to the cell, during both the effective and the recovery stroke. For future reference, it is convenient to specify both these vectors and $\boldsymbol{n}$ and $\boldsymbol{t}$ (equation (2.4)) in terms of unit vectors $\boldsymbol{p}, \boldsymbol{q}$ fixed in the cell (see figures 4 and 5).

The unit vectors normal and tangential to an element on the right-hand flagellum are given by

$$\boldsymbol{n} = \sin\chi\,\boldsymbol{p} - \cos\chi\,\boldsymbol{q} \tag{5.5}$$

and

$$\boldsymbol{t} = \cos\chi\,\boldsymbol{p} + \sin\chi\,\boldsymbol{q}. \tag{5.6}$$

The position of an element on the right flagellum relative to the centre of the cell during the effective stroke is given by

$$\boldsymbol{r} = a\,\boldsymbol{p} + s\,\boldsymbol{t} = (a + s\cos\chi)\,\boldsymbol{p} + s\sin\chi\,\boldsymbol{q}, \tag{5.7}$$

where χ is the angle between the flagellum and the body axis $\boldsymbol{p}$ (see figure 4*a*). During the effective stroke the element moves through a right angle in time T_e. The angular velocity of the flagellum is then given by

$$\dot{\chi} = \frac{\pi}{2}\frac{1}{T_e}. \tag{5.8}$$

The velocity of the flagellar element is then given by

$$\dot{\boldsymbol{r}} = -s\dot{\chi}\sin\chi\,\boldsymbol{p} + s\dot{\chi}\cos\chi\,\boldsymbol{q}. \tag{5.9}$$

To obtain corresponding vectors for an element on the left flagellum, change the angle χ to $-\chi$.

During the recovery stroke, a bending wave propagates up the length of the flagellum, l, at a constant velocity, w say. Thus, the recovery stroke takes w/l seconds to occur. We consider the recovery stroke in two parts: the section parallel to the body axis $\boldsymbol{p}$ and the section changing angle and retreating towards the body axis (figure 4*b*). The position of an element on the right flagellum in the section parallel to the body axis is given by

$$\boldsymbol{r} = (a+s)\,\boldsymbol{p} \tag{5.10}$$

with $\boldsymbol{t} = \boldsymbol{p}$ and $\boldsymbol{n} = -\boldsymbol{q}$. The straight section is of length wt where $wt < l$. This element is stationary with respect to the centre of the organism O. The position of an element in the angled segment on the right flagellum is given by

$$\boldsymbol{r} = (a+wt)\,\boldsymbol{p} + (s-wt)\,\boldsymbol{t} = [a+wt+(s-wt)\cos\chi]\,\boldsymbol{p} + (s-wt)\sin\chi\,\boldsymbol{q}, \tag{5.11}$$

where $\frac{1}{2}\pi \leqslant \chi \leqslant \pi$ and $t = 0$ is taken at the start of the recovery stroke. The velocity of the flagellum is then given by

$$\dot{\boldsymbol{r}} = [w(1-\cos\chi) - (s-wt)\dot{\chi}\sin\chi]\,\boldsymbol{p} + [-w\sin\chi + (s-wt)\dot{\chi}\cos\chi]\,\boldsymbol{q}. \tag{5.12}$$

The angular velocity of the flagellum is calculated in one of two ways. If we assume that the angle decreases with constant angular velocity during the stroke and that the flagellum bends through a right angle, it thus has angular velocity

$$\dot{\chi} = \frac{\pi}{2}\frac{w}{l}. \tag{5.13}$$

In the second model for the flagellar angular velocity, we calculate the moment of viscous forces about the bending point, by using resistive-force theory and ignoring the presence of the cell body (Appendix A). The angular velocity of the flagellum is then chosen to give zero moment. The resulting equation for the angular velocity is

$$\dot{\chi} = \frac{3}{2}\frac{w\sin\chi}{(l-wt)}. \tag{5.14}$$

The results of using both methods will be given.

It can now be seen that the time taken for the effective stroke is given by

$$T_e = T - \frac{w}{l}, \tag{5.15}$$

where T is the total time for one beat. Time, though, merely acts as a parameter within the model. The amount of time taken by the effective stroke in comparison with the recovery stroke has no effect upon the average velocity and angular velocity of the organism if the total time for one beat remains constant. This is a consequence of the zero Reynolds-number-flow assumption.

To obtain the total force and torque upon each flagellum it is necessary to integrate (2.4) and its vector product with $\boldsymbol{r}$, incorporating (2.5) to (3.1) with either (3.2) or (3.3) and using (5.5) and (5.6), along the flagellum from the base to the tip; $s = 0$ to $s = l$. For the effective stroke, a simple integration is required for each term, while for the recovery stroke, a choice of (5.13) or (5.14) for use in (5.12) will be necessary along with two integrals, from 0 to wt and from wt to l.

Finally, the vector equations for the total force and torque, (2.1) and (2.2), reduce in our uniplanar system to three simultaneous equations in three unknowns:

$$\alpha_1 v_p + \alpha_2 e \cos(2\theta) = \alpha_3, \tag{5.16}$$

$$\alpha_4 v_q + \alpha_5(\dot{\theta} + \omega/2) + \alpha_6 e \sin(2\theta) = 0, \tag{5.17}$$

and

$$\alpha_7 v_q + \alpha_8(\dot{\theta} + \omega/2) + \alpha_9 e \sin(2\theta) = -mgh \sin(\theta - \gamma), \tag{5.18}$$

where v_p and v_q are the components of the organism's translational velocity parallel and perpendicular to the body axis $\boldsymbol{p}$ respectively, $\dot{\theta}$ is the angular velocity of the organism, and α_1 to α_9 are dimensional, time-dependent coefficients that depend only on the parameters of the flagellar beat.† The variables v_p, v_q and $\dot{\theta}$ are the unknowns in the equations which may be solved at any time throughout the beat. The results are then integrated with respect to time to give $\boldsymbol{V}$ and $\boldsymbol{\Omega}$, the average velocity and average angular velocity of the organism over the beat.

From (5.16), it can be seen that the velocity of the organism in the primary body direction, v_p, is uncoupled from the equations for the transverse velocity and the angular velocity. This is an expected consequence of the planar flagellar beat since contributions to the torque equation from a force acting in the direction of motion upon identically beating flagella produce identical contributions but of opposite sign, resulting in zero net effect. A force acting perpendicular to the direction of motion will produce identical contributions on two flagella but of the same sign, resulting in the appearance of the v_q term in the viscous torque equation.

During the calculation of the results, we have assumed that, although $\dot{\theta}$ is often non-zero, the angle θ is constant throughout the beat. From (5.17) and (5.18), it is possible to solve for the angular velocity explicitly:

$$\dot{\theta} = -\omega/2 - \left(\frac{\alpha_6\alpha_7 - \alpha_4\alpha_9}{\alpha_5\alpha_7 - \alpha_4\alpha_8}\right) e \sin(2\theta) + \left(\frac{\alpha_4}{\alpha_5\alpha_7 - \alpha_4\alpha_8}\right) mgh \sin(\theta - \gamma). \tag{5.19}$$

Solution of this differential equation will show how the angle θ, and hence $(\theta - \gamma)$, changes throughout the beat, and we shall be able to identify the conditions under which this change can be neglected. Moreover, the time-dependent coefficients are laborious to calculate at each time step. We shall therefore also examine the accuracy of replacing them by their average values in the calculation of the velocity and angular velocity.

In the case of zero strain rate, the angles θ and γ are not defined and it is the angle between $\boldsymbol{p}$ and $\boldsymbol{k}$, say β, that should be considered and should replace $\theta - \gamma$ in the last term of (5.19) (see figure 5). Equation (5.19) is analogous in our model to the angular velocity equation found by Pedley & Kessler (1987) for a spheroidal cell without flagella ((1.1) above). The inclusion of the flagellar torque causes the coefficients of strain and gravity to be more complicated than the quantities α_0 and B which they replace. Though the new equation as yet lacks three-dimensional generality, it will improve the calculation of the angular velocity of the organism through the inclusion of the torque due to the flagellar beat. In particular, the ambient strain rate, e, which has no effect on a spherical cell body, does have an influence on a flagellated cell even when its body is spherical.

† The expressions defining them are lengthy and of no intrinsic interest; a list has been deposited in the JFM editorial office.

	Any cell	*Chlamydomonas*	Standard value used here
Cell diameter	2–500 μm	4–20 μm	10 μm
Flagellar length	5–200 μm	4–20 μm	10 μm
Flagellar diameter	0.2 μm		0.2 μm
Beat frequency	5–100 Hz	40–60 Hz	50 Hz
Cell density		1.01–1.10 g cm^{-3}	1.05 g cm^{-3}
Centre of gravity offset		0–0.05 body diameters	0.1 μm
Swimming speed	10–500 μm s^{-1}	0–200 μm s^{-1}	To be calculated

TABLE 1

6. Results

Firstly, we estimate the model parameters, using published data, and then we calibrate the model by comparing its prediction for pure up-swimming in a still fluid to the observations of Ruffer & Nultsch (1985). Then, the model is used to predict the angular velocity of the organism in other conditions.

6.1. *Typical data values*

Table 1 gives typical data ranges for arbitrary flagellated cells from Holwill (1982), for *Chlamydomonas* from Kessler (1986), and the standard values used in obtaining the results which follow; other values will also be used to test the model's sensitivity to the parameters.

The majority of results are given in non-dimensional form. The characteristic length scale is the body diameter and the characteristic time scale is the time for one beat. Velocities consequently are given in terms of body diameters per beat. Specific results have been dimensioned to give comparisons with the data in the table.

6.2. *Vertical up-swimming*

Comparison between the model and experimental observation is easiest in the case of vertical up-swimming. That is, *Chlamydomonas reinhardtii* have been observed swimming vertically upwards (on average) and measurements of their mean upward velocity have been taken (Ruffer & Nultsch 1985). This is somewhat different from the mean speed at which cells swim relative to the suspending medium, because their swimming direction is randomly distributed; this too has been measured, at least for *C. nivalis* (Kessler, Hill & Häder 1992). In our model, pure up-swimming corresponds to the organism swimming in a stationary flow field, one without vorticity or strain rate or gravitational torque.

6.2.1. *Comparison of resistance coefficients*

It was seen in §3 that the resistance coefficients, K_N and K_T depend on the ratio between the length, l, of the flagellum and its radius, b. Thus, in figure 6, the abscissa, K_N/K_T, is a function of l/b. The different curves on the graph are for different values of the flagellar length which has been non-dimensionalized by the body diameter. Thus, for any organism, if the ratios of flagellar length to body diameter and flagellar radius to flagellar length are known then the predicted vertical up-swimming velocity is shown.

For *Chlamydomonas*, the flagellar thickness is about 0.02 of the flagellar length and the flagellar length is approximately equal to the body diameter. Using Gray

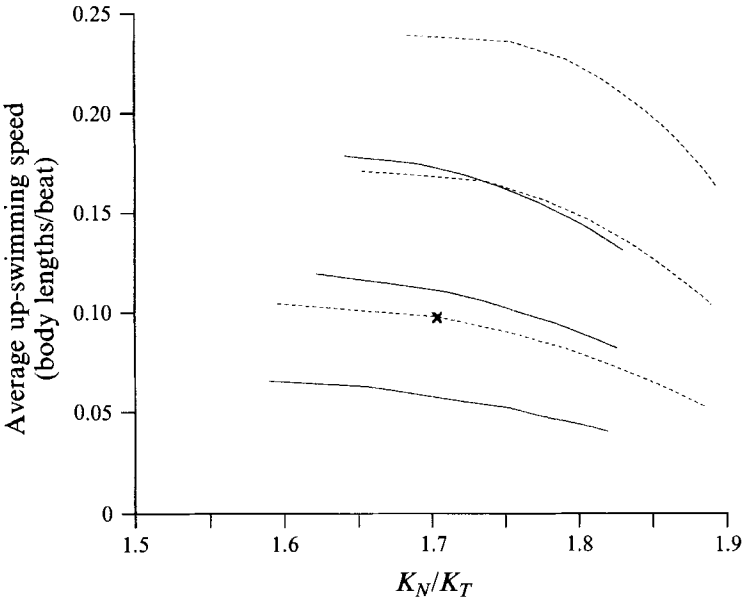

FIGURE 6. Up-swimming speed plotted against K_N/K_T for varying flagella lengths ($l = 2a$ (bottom), 3a,4a (top), where a is the body radius). Dashed lines are speeds found using Lighthill's (1976) coefficients, the solid lines those using Gray & Hancock's (1955) coefficients. Flagellar thickness increases as $K_N/K_T \to 0$. The cross marks the speed for the parameter values of our chosen organism.

& Hancock's coefficients, we predict a velocity of 0.06 body diameters per beat or 31 μm s^{-1}if the body diameter is 10 μm and the organism beats at a frequency of 50 s^{-1}. On the other hand, using Lighthill's coefficients, we predict a velocity of 0.10 body diameters per beat or 50 μm s^{-1}.

Both these values are in the range of observed swimming speeds, as seen in table 1. Johnson & Brokaw (1979) found that Lighthill's coefficients gave better agreement with slender-body theory when the body-to-flagellar length ratio is comparable. As this is the case in this model, we choose to use Lighthill's coefficients in deriving the remainder of the results, i.e. $K_N = 3.7$ and $K_T = 2.2$.

6.2.2. *Velocity variation during the beat*

Figure 7 shows how the velocity of the organism is predicted to change over the beat. In the first part of the beat, the organism is performing the effective stroke. It swims forward with increasing velocity as the stroke progresses. At the end of the stroke there is a distinct change from effective to recovery stroke causing a discontinuity in the velocity. During the recovery stroke, the organism swims backwards with an approximately constant but smaller velocity. A small minimum is seen in the velocity at the point where the furthest extent of the flagella is closest to the cell body.

The velocities in the recovery stroke have been calculated in two different ways, as stated before: assuming the angular velocity for zero-moment or constant angular velocity. It can be seen that, though the backwards velocity is initially greater, the zero-moment angular velocity model results in a slightly smaller backwards velocity than the constant angular velocity model throughout the majority of the recovery stroke, and hence in a smaller net backwards displacement.

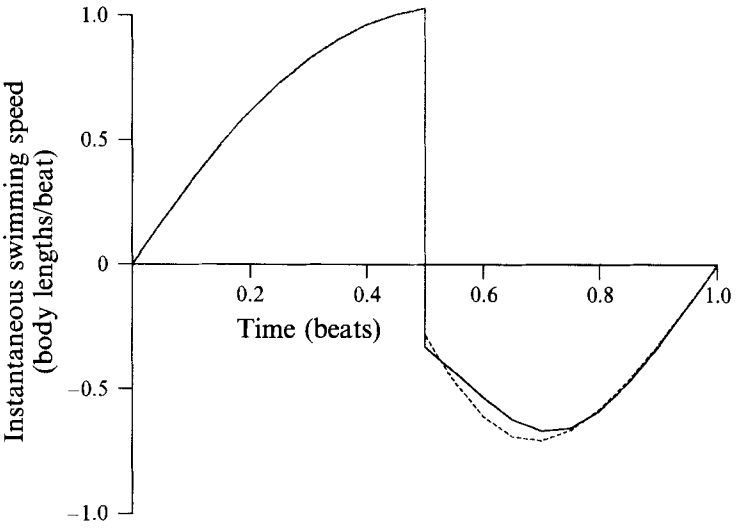

FIGURE 7. Variation in up-swimming speed during one flagellar beat. Discontinuity occurs at changeover between effective stroke ($v > 0$) and recovery stroke ($v < 0$). Solid line in recovery stroke shows the result of using the zero-moment method of calculating flagellar angular velocity.

An organism with flagellar length equal to body diameter was found to swim upwards for a distance of about 0.33 body diameters in the effective stroke and to regress about 0.23 body diameters during the recovery stroke. This gives an average swimming velocity of 0.10 body diameters per beat. When comparing the two methods described for the recovery stroke, the zero-moment angular velocity model gave an average swimming velocity of 0.10 body diameters per beat and the constant angular velocity method gave the average swimming speed as 0.09 body diameters per beat.

In the following results, the zero-moment model will be used throughout.

6.3. *Calculation of angular velocity*

The main application of a model such as this will be in the calculation of angular velocity for use in a continuum model of a suspension of cells. We thus consider the new model's predictions for angular velocities, and compare them with the earlier predictions of Pedley & Kessler (1987) which ignored the presence of the flagella.

6.3.1. *Gravitational torque only*

Assuming no ambient flow, then if the organism is swimming at an angle β to gravity, equivalent to $\theta - \gamma$ in (5.19), there will exist a re-orientating torque due to gravity only. The viscous torque on the body and the flagella will balance the gravitational torque opposing the angular velocity $\dot{\beta}$. The inclusion of the flagella will enhance the magnitude of this viscous torque and will therefore result in a lower value for the angular velocity than an equation excluding them. Figure 8 shows the difference. The results were calculated for flagellar length equal to the body diameter. The angular velocity values obtained by including the flagellar torque are 50% lower than without it. This is a significant difference which may partly be explained by the choice of an idealized flagellar beat pattern. We feel, though, that the flagellar torque, whichever form the beat pattern takes, will be a significant term affecting the calculation of the angular velocity.

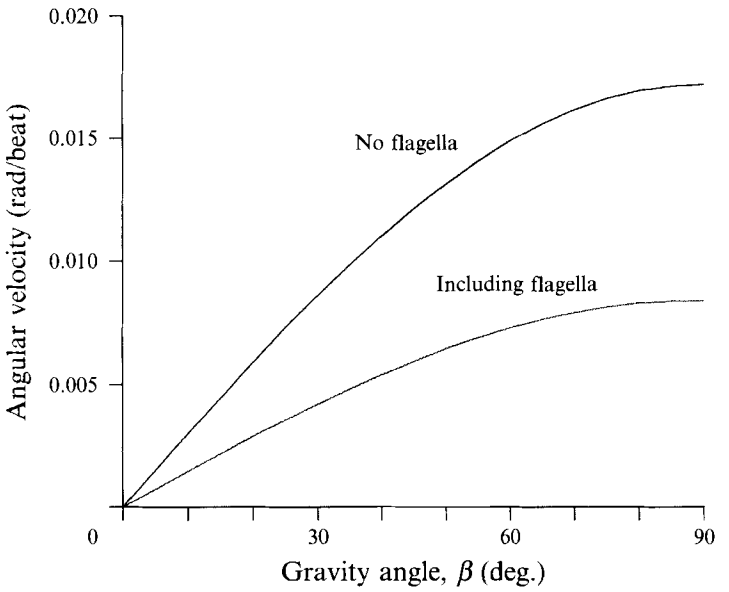

FIGURE 8. Plots of angular velocity driven by gravitational torque only, against gravity angle, showing the effects of neglecting the flagella.

In order to decide whether it is valid to neglect the variation in β during the beat, when calculating $\dot{\beta}$, a tolerance was decided upon. If the maximum change in β is less than this, we consider the calculation to be accurate.

Equation (5.19) (with $\omega = e = 0$ and $\beta = \theta - \gamma$) was solved numerically for $\beta(t)$ using a fourth-order Runge–Kutta scheme. The integration was performed in two ways: (*a*) using the instantaneous values for the time dependent coefficients and (*b*) by an approximate method in which the average values for the coefficients were used. If sufficiently accurate this may provide an efficient approximation in cases when it is not valid to neglect the variation of β or θ during a beat. Figure 9 shows how, over one beat, the angle β changes under the influence of a gravitational torque only, when the value of β in the equation was take to be 40°. The use of average values for the time-dependent coefficients instead of the full calculations shows the greatest difference at the changeover from effective to recovery stroke but agreement is generally good throughout the beat. Despite (5.19) being nonlinear, use of the average values for the coefficients leads to a very accurate estimate of average angular velocity (equivalent to the total angular displacement in one beat).

For a 40° displacement from gravity, the angle moves to 39.7° at the end of one beat for the parameter values chosen here, so neglect of this variation is certainly justified.

6.3.2. *Shear flow*

We have examined the assumption that the angle between the body axis and a fixed axis (gravity) remains constant throughout the beat when the only torque acting is gravitational. We found that the deviation was small over the beat.

Now, we examine the rotation of the organism for more complicated flows involving both rate of strain and vorticity. We define a new notation for the coefficient

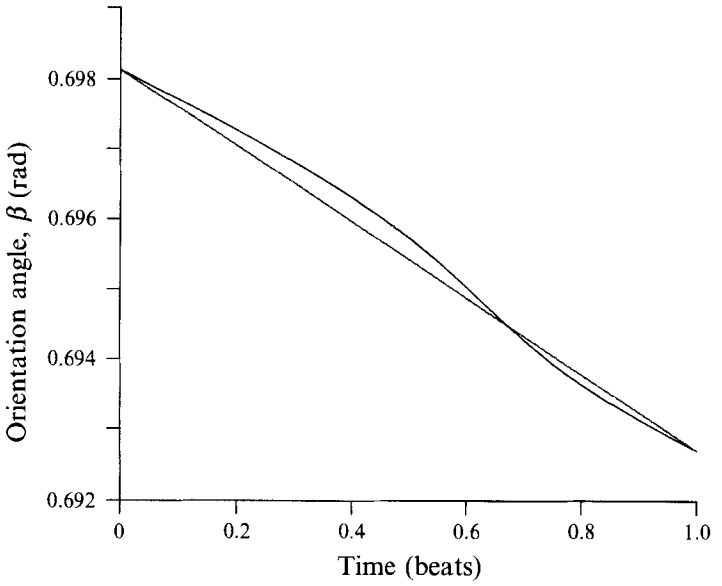

FIGURE 9. Change in orientation angle β during one beat. Gravity acting at 40° ($\beta = 40°$ at $t = 0$). Straight line shows the effect of using average values for the time-dependent coefficients.

functions in (5.19) as

$$\eta = \left(\frac{\alpha_4}{\alpha_4\alpha_8 - \alpha_5\alpha_7} \right) \tag{6.1}$$

and

$$\zeta = \left(\frac{\alpha_6\alpha_7 - \alpha_4\alpha_9}{\alpha_4\alpha_8 - \alpha_5\alpha_7} \right). \tag{6.2}$$

Note that ζ is non-dimensional while η has units of $\mathrm{kg^{-1}m^{-2}s}$ and both are positive-valued functions. Then (5.19) becomes

$$\dot{\theta} = -\tfrac{1}{2}\omega + \zeta e \sin(2\theta) - \eta mgh \sin(\theta - \gamma). \tag{6.3}$$

The previous results show that it is accurate to replace η by its average value $\bar{\eta}$. We can use this to calculate a critical value for the vorticity, $|\omega|$, below which the change in θ during the beat may be neglected. If the organism was placed in a flow containing only vorticity, $e = 0$, and was swimming horizontally, with $\beta = \frac{1}{2}\pi$ so that the gravitational torque is maximal and in the same sense as the viscous torque for $\omega > 0$ (see figure 5), then putting $\dot{\theta} = -\dot{\theta}_{\max}$ in (6.3) gives the maximum permissible value of the vorticity:

$$\omega_{\max} = 2(\dot{\theta}_{\max} + \bar{\eta} mgh). \tag{6.4}$$

We decided arbitrarily that an angular displacement of 5° (0.087 rad) per beat was the maximum tolerable variation in θ. For the specification of the organism described above, $\bar{\eta} mgh = 0.008$. Hence, this gives the maximum vorticity allowable as $\omega_{\max} = 9.5\ \mathrm{s^{-1}}$.

A different simplification is possible when $|\omega|$ exceeds the allowable value, for then the term $-\omega/2$ dominates the other terms on the right-hand side of (6.3), and, to a good approximation, the cell rotates with the ambient fluid. In such a vigorous flow, the details of how the organism swims are likely to be unimportant.

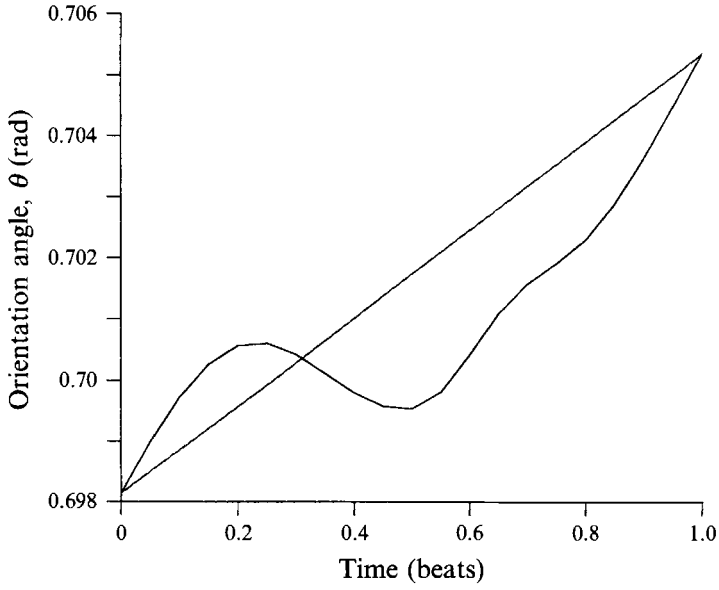

FIGURE 10. Change in orientation angle θ during one beat. Pure straining motion ($e = 10\,s^{-1}$) initially acting at $40°\theta = 40°$ at $t = 0$) with no gravitational torque ($\theta - \gamma = 0$ at $t = 0$). Straight line shows the effect of using the average values for the time-dependent coefficients.

At this stage, we can perform a similar analysis for pure straining flow. If there was no vorticity acting, $\omega = 0$, and initially the organism was swimming vertically upwards, $\theta - \gamma = 0$, then the major influence upon the orientation of the organism would be the rate of strain. Figure 10 shows how, over one beat, the angle θ changes in the situation described above. Equation (6.3) was solved numerically using the instantaneous values of η and ζ and using their average values, $\bar{\eta}$ and $\bar{\zeta}$ respectively. Unlike the gravitational case, the organism exhibits a large angular variation during one beat. The average value, while not being as accurate within the beat, does give a good approximation for the total angular displacement in one beat. With θ initially $40°$ and $e = 10\ s^{-1}$, after one beat θ has moved to $40.4°$. The average angular velocity is very small, about $5°\ s^{-1}$ for a strain rate of $10\ s^{-1}$, with the difference between using the instantaneous value or the average value being small up to extremely large values of the rate of strain.

So, we cannot use the average value if we wish to examine the variation within a beat but may use the average value if the mechanics of the beat are not important. In most applications, the organism will be placed in a flow in which the rate of strain is of comparable size to the vorticity.

We can calculate a similar maximum value of the rate of strain for which the model holds. The maximum value of the rate of strain occurs when $\theta = \frac{1}{4}\pi$. If we ignore any vorticity ($\omega = 0$), assume that gravity is acting with maximum effect in the same direction as the rate of strain ($\gamma = -\theta$), then putting $\dot{\theta} = -\dot{\theta}_{\max}$ again gives the maximum allowable rate of strain,

$$e_{\max} = \frac{(\dot{\theta}_{\max} + \bar{\eta} mgh)}{\bar{\zeta}}. \tag{6.5}$$

Hence substituting for $\bar{\eta}mgh$ and $\dot{\theta}_{\max}$ as before and with $\bar{\zeta} = 0.09$ for our typical organism, we obtain a maximum rate of strain of $e_{\max} = 52\ \mathrm{s}^{-1}$.

Note that since we have assumed that the organism's body is spherical, the rate of strain exerts a torque only upon the flagella. This torque is considerably smaller than that exerted by a comparable vorticity on the body. We expect the effect of the strain to be considerably greater on a spheroidal body.

7. Discussion

Previous papers have shown that resistive-force theory can be used to calculate a spermatazoon's velocity accurately when the cell body is ignored. In this paper, we have incorporated the body into the model by considering its influence on the flow past the flagella, and have thereby been able to model an organism for which the flagellar length is comparable to the body length. We also included the flagellar torque in the torque balance equation and provided an idealized model for the flagellar beat.

Despite the reservations about the use of resistive-force theory, the model shows good qualitative agreement with observation in its calculation of swimming velocity. It does show also that the flagellar torque can have a significant effect upon the angular velocity, which can be significantly over-estimated if the flagella are ignored. When calculating the angular velocity, the time dependence of the beat coefficients would make the use of our method laborious, but we have shown that using the average values of these coefficients, (6.1)–(6.2), is sufficiently accurate.

The average values of the time-dependent beat coefficients were shown to be very accurate in the case of gravitational torque. For pure straining flow, however, the flagellar beat is highly important since there will be no effect upon the spherical body and the strain acts entirely through the flagella. Though the average values may also be used in this case, the change in the angular displacement during straining flow was shown to be more variable over the beat than during gravitational torque.

We have also shown that the assumption that the organism's orientation does not change significantly during one beat is valid up to a maximum value of vorticity or rate of strain (in our case, with a spherical body, the effect of the vorticity in the ambient flow is much greater than that of the strain rate). However, if the organism is rotating too rapidly for the orientation to be assumed constant over one beat, it is unlikely that the details of the organism's swimming will be important anyway.

As stated earlier, Pedley & Kessler's (1992) general equation for the angular velocity of an organism in a shear flow, (1.1), is analogous, in the case described above, to (5.19). We can carry this analogy over to the definition of the constants in the two equations. Comparisons show that the cell's eccentricity parameter α_0 (in Pedley & Kessler's notation) is, in the new equation, given by

$$\alpha_0 = \bar{\zeta}. \tag{7.1}$$

In addition, defining η^* to be a non-dimensional η †, the gravitational re-orientation time becomes

$$B = \frac{3\mu v}{8\pi\bar{\eta}^* mgh} \tag{7.2}$$

† Non-dimensionalization: $\eta = \eta^*/\mu a^3 = 4\pi\eta^*/3\mu v$ using the assumption that the body is spherical.

so that Pedley & Kessler's coefficient $\alpha_\perp$ is given by

$$\alpha_\perp = \frac{3}{4\pi\bar{\eta}^*}. \tag{7.3}$$

Substitution of the new values into the existing equation will therefore improve the continuum models, which are based on these equations, for the cases in which the new values are valid, i.e. in which the cells are not rotating too rapidly.

Using the idealized beat pattern of § 4.2 with the typical organism dimensions given in table 1, we obtain $\bar{\zeta} = \alpha_0 = 0.09$ and $\eta^* = 0.019$, so $\alpha_\perp = 12.6$.

The value of α_0 chosen by Pedley & Kesler (1990) was 0.31, based on visual examination of dead cells under a microscope. The cell bodies were taken to be spheroidal with no flagella. Our value was based upon a spherical cell body (for which $\alpha_0 = 0$) with flagella. The results suggest that the value of α_0 for a spheroidal cell with flagella would approach the sum of the two previous values, i.e. 0.40; we are performing a more detailed calculation to confirm this.

The corresponding value of $\alpha_\perp$, for spheroidal cells with $\alpha_0 = 0.31$, is 6.8, leading to a gyrotactic reorientation time (B) of 3.4 s (Pedley & Kessler 1990). Our value of 12.6 gives $B \approx 6.3$ s. The slower reorientation is not surprising because the flagellar torque acts as an extra brake on the angular velocity of the organism. This means that, while the organism rotates more slowly than predicted by ignoring the presence of the flagella, it is more resistant to any large impulses that may influence it through the far-field flow. Any large vorticity or rate of strain that act for a short period of time on the organism would result in a lower angular velocity, and hence a lower angular deviation from the organism's preferred path, than one would suppose when modelling the organism without the flagella.

The analysis of this paper is a first step. Spheroidal bodies and three-dimensional flows will be considered in subsequent papers leading to a description of the motion of a general biflagellate organism beating in a general flow.

M. S. Jones is funded by an earmarked EPSRC award.

Appendix. Calculation of zero-moment angle

A cell is performing the recovery stroke (figure 7). A point on the flagellum, P, is travelling in the body direction, **p**, with constant velocity w. We take $t = 0$ at the start of the recovery stroke. At time t, points on the flagellum below P ($s \leqslant wt$) are in their initial position for the start of the effective stroke and so have ceased moving with respect to P. Points on the flagellum above P ($s > wt$) are rotating with angular velocity, $\dot{\chi}$ about P as they retreat back to their initial point for the effective stroke. A point on the flagellum above P has a position vector $\boldsymbol{r}$ given by (5.11).

At this stage, we use resistive-force theory, (2.4), to calculate the viscous force acting on the element $\boldsymbol{t}ds$ of the flagellum at the point $\boldsymbol{r}$, and hence the viscous torque about the point P, for the case where the only motion is the beating of the flagella. That is, we neglect the fluid flow and the presence of the cell body, and set $\boldsymbol{u}_{\rm rel} = -\dot{\boldsymbol{r}}$, given by (5.12). For the calculation of the torque, only the normal component of $\boldsymbol{u}_{\rm rel}$ is required, i.e.

$$(\dot{\boldsymbol{r}} \cdot \boldsymbol{n}) = -(s - wt)\dot{\chi} + w \sin\chi, \tag{A 1}$$

since $\boldsymbol{n}$ is given in terms of $\boldsymbol{p}$ and $\boldsymbol{q}$ by (5.5).

The total normal moment about P, M_n, from all the elements with $s > wt$ is given by

$$M_n = \int_{wt}^{l} (\boldsymbol{F} \cdot \boldsymbol{n})(s - wt)\mathrm{d}s \tag{A 2}$$

or

$$M_n = \int_{wt}^{l} K_N(-(s - wt)\dot{\chi} + w \sin\chi)(s - wt)\mathrm{d}s. \tag{A 3}$$

Integrating and then setting $M_n = 0$ gives

$$\dot{\chi} = \frac{3}{2}\frac{w \sin\chi}{(l - wt)}, \tag{A 4}$$

which is positive. Hence, $\dot{\chi}$ is the angular velocity of the flagellum about the pivot point P such that the moment in the normal plane is zero.

Note that (A 4) can be integrated to give

$$\chi = 2\tan^{-1}\left[\left(1 - \frac{wt}{l}\right)^{-3/2}\right], \tag{A 5}$$

which indeed starts at $\chi = \frac{1}{2}\pi$ when $t = 0$, and finishes at $\chi = \pi$ when $t = l/w$, just as in the constant angular velocity case.

REFERENCES

Brokaw, C. J. & Luck, D. J. L. 1983 Bending patterns of *Chlamydomonas* flagella: I Wild type bending patterns. *Cell Motility.* **3**, 131–150.

Fauci, L. J. & Peskin, C. S. 1988 A computational model of aquatic animal locomotion. *J. Comput. Phys.* **77**, 85–108.

Gray, J. & Hancock, G. J. 1955 The propulsion of sea-urchin spermatozoa. *J. Exp. Biol.* **32**, 802–814.

Higdon, J. J. L. 1979 A hydrodynamic analysis of flagellar propulsion. *J. Fluid Mech.* **90**, 685–711.

Holwill, M. E. J. 1982 Dynamics of flagellar movement. In *Symposia of the Society for Experimental Biology: Prokaryotic and Eukaryotic Flagella.* vol. 35, pp. 289–312.

Hyams, J. S. & Borissy, G. G. 1978 Isolated flagellar apparatus of *Chlamydomonas*: Characterization of forward swimming and alteration of waveform and reversal of motion by calcium ions in vitro. *J. Cell Sci.* **33**, 235–253.

Jeffery, G. B. 1922 The motion of ellipsoidal particles immersed in a viscous fluid. *Proc. R. Soc. Lond.* A **102**, 161–79.

Johnson, R. E. & Brokaw, C. J. 1979 Flagellar hydrodynamics: A comparison between resistive-force theory and slender-body theory. *Biophys. J.* **25**, 113–127.

Kessler, J. O. 1985 Co-operative and concentrative phenomena of swimming micro-organisms. *Contemp. Phys.* **26**, 147–166.

Kessler, J. O. 1986 Individual and collective dynamics of swimming cells. *J. Fluid Mech.* **173**, 191–205.

Kessler, J. O., Hill, N. A. & Häder, D. P. 1992 Orientation of swimming flagellates by simultaneously acting external factors. *J. Phycology* **28**, 816–822.

Kim, S. & Karrila, J. S. 1991 *Microhydrodynamics: Principles and Selected Applications.* Butterworth-Heinemann.

Lighthill, J. 1976 Flagellar hydrodynamics. *SIAM Rev.* **18**, 161–230.

Pedley, T. J., Hill, N. A. & Kessler, J. O. 1988 The growth of bioconvection patterns in a uniform suspension of gyrotactic micro-organisms. *J. Fluid Mech.* **195**, 223–237.

Pedley, T. J. & Kessler, J. O. 1987 The orientation of spheroidal micro-organisms swimming in a flow field. *Proc. R. Soc. Lond.* B **231**, 47–70.

PEDLEY, T. J. & KESSLER, J. O. 1990 A new continuum model for suspensions of gyrotactic micro-organisms. *J. Fluid Mech.* **212**, 155–182.

PEDLEY, T. J. & KESSLER, J. O. 1992 Hydrodynamic phenomena in suspensions of swimming micro-organisms. *Ann. Rev. Fluid Mech.* **24**, 313–358.

PHAN-THIEN, N., TRAN-CONG, T. & RAMIA, M. 1987 A boundary element analysis of flagellar propulsion. *J. Fluid Mech.* **184**, 533–549.

RAMIA, M. 1991 Numerical model for the locomotion of spirilla *Biophys J.* **60**, 1057–1078.

RAMIA, M., TULLOCK, D. L. & PHAN-THIEN, N. 1993 The role of hydrodynamic interaction in the locomotion of micro-organisms *Biophys. J.* **65**, 755–778.

RINGO, D. L. 1967 Flagellar motion and fine structures of the flagellar apparatus in *Chlamydomonas. J. Cell Biol.* **33**, 543–571.

RUFFER, U. & NULTSCH, W. 1985 High speed cinematographic analysis of the movement of *Chlamydomonas. Cell Motility* **5**, 251–263.

WINET, H. & JAHN, T. L. 1972 On the origin of bioconvection fluid instabilities in *Tetrahymena* culture systems. *Biorheol.* **9**, 87–94.